*Carbohydrate Research*, 221 (1991) 63–81
Elsevier Science Publishers B.V., Amsterdam



# Characterisation by $^1$H-n.m.r. spectroscopy of oligosaccharides, derived from arabinoxylans of white endosperm of wheat, that contain the elements →4)[α-L-Ara*f*-(1→3)]-β-D-Xyl*p*-(1→ or →4)[α-L-Ara*f*-(1→2)][α-L-Ara*f*-(1→3)]-β-D-Xyl*p*-(1→

Rainer A. Hoffmann, Bas R. Leeflang, Martina M. J. de Barse, Johannis P. Kamerling, and Johannes F. G. Vliegenthart*
*Bijvoet Center, Department of Bio-Organic Chemistry, Utrecht University, P.O. Box 80.075, 3508 TB Utrecht (The Netherlands)*

(Received January 30th, 1991; accepted for publication May 10th, 1991)

ABSTRACT

The structure of penta- to hepta-saccharides, generated by digestion of purified wheat-endosperm arabinoxylan with endo-(1→4)-β-D-xylanase and isolated by gel-permeation chromatography on Bio-Gel P-6 followed by high-performance anion-exchange chromatography with pulsed amperometric detection, was established using monosaccharide and methylation analysis, f.a.b.-m.s., and $^1$H-n.m.r. spectroscopy. The oligosaccharides had a core of (1→4)-linked β-D-xylopyranosyl residues 3- or 2,3-substituted with single α-L-arabinofuranosyl groups, and gave $^1$H-n.m.r. spectra typical for each type.

## INTRODUCTION

Arabinoxylans are found, among other polysaccharides, in the endosperm of such cereals as wheat[1–3], oat[4], barley[5], rye[6], and rice[7]. Wheat-endosperm arabinoxylans consist of a (1→4)-linked backbone of β-D-Xyl*p* residues that are variously unsubstituted, 3- and 2,3-disubstituted[8–10]. Single α-L-Ara*f* groups occur[9,10] as substituents, but the methylation analysis data do not exclude a small percentage of 2-, 3-, or 5-substitution[10]. There is evidence[10–12] for the occurrence of a 3-substituted, but not a 2,3-substituted, β-Xyl*p* residue in arabinoxylan oligosaccharides. Little is known about the distribution of α-L-Ara*f* groups along the xylan core. Endo-(1→4)-β-D-xylanases from different sources may be used for the degradation of the arabinoxylans, but they can vary in specificity and thereby yield different mixtures of oligosaccharides. We have used a purified endo-(1→4)-β-D-xylanase from an *Aspergillus* species to degrade a wheat arabinoxylan and have characterised the resulting oligosaccharides by 1D and 2D (HOHAHA and ROESY) 500- and 600-MHz $^1$H-n.m.r. spectroscopy.

* To whom correspondence should be addressed.

0008-6215/91/$03.50 

EXPERIMENTAL

*Preparation of (1→4)-linked β-D-xylo-oligosaccharides.* — The water-soluble part (1 g) of commercial oat-spelt xylan[4] (Fluka) was partially hydrolysed with 3.5mM HCl (100 mL) for 16 h at 85° under $N_2$. The precipitated xylan (200 mg), which contained Xyl, Ara, and Glc in the molar ratios 93:1:2, was collected by centrifugation at 13,000*g*, washed twice with distilled water, lyophilised, and partially hydrolysed with 0.1M HCl (12 mL) for 5 h at 85° under $N_2$. After centrifugation at 13,000*g*, the supernatant solution was lyophilised to yield a mixture (81 mg) of xylose and xylo-oligosaccharides, which was fractionated on a column (100 × 1.4 cm) of Bio-Gel P-2 (Bio-Rad) by elution with water. Fractions with a d.p. of up to 8 were further purified by high-performance anion-exchange chromatography (see below). The molecular weights of the compounds of fractions **1–7** were established by positive-ion f.a.b.-m.s.

*Preparation of arabinoxylan oligosaccharides.* — The arabinoxylan fraction[9] L-$PP_{44}$ (370 mg), isolated from the tailing fraction of the white flour of the soft wheat variety Kadet, was dissolved in 50mM $NH_4OAc$ buffer (pH 5.5, 200 mL) and the solution was incubated for 16 h at 37°, with two aliquots of an *Aspergillus* endo-(1→4)-β-D-xylanase (500 μL; 2 × $10^5$ U/mL, 1 U = 1 μg of xylose release/min at 40°, pH 5.0) being added after 0 and 4 h. Cellulase, alpha-amylase, arabinase, and protease activities were not detectable in the enzyme preparation. The solution was then cooled to 4°, passed through a column (20 × 2 cm) of Dowex 50W-X8 ($H^+$) resin (100–200 mesh, Bio-Rad) at 4°, and lyophilised. The mixture of oligosaccharides was fractionated in four portions of 90 mg on a column (100 × 2.5 cm) of Bio-Gel P-6 (200–400 mesh, Bio-Rad) by elution with water (24 mL/h, 4.0-mL fractions), and refractive-index monitoring.

*High-performance anion-exchange chromatography with pulsed amperometric detection (h.p.a.e.–p.a.d.).* — A Dionex Bio-LC quaternary gradient module was used, equipped with a model PAD-2 detector, a preparative CarboPac PA-1 column (250 × 9.0 mm), and a Shimadzu C-R6A recorder/integrator. The detection by p.a.d. with a gold working electrode and triple-pulse amperometry[13] comprised the following pulse potentials and durations: $E_1$ 0.05 V, 300 ms; $E_2$ 0.65 V, 120 ms; $E_3$ −0.95 V, 60 ms. The response time of the p.a.d. was set to 1 s. Samples were dissolved in $H_2O$ (500 μL) and applied in five 100-μL portions. Elutions were carried out with eluent *A* (0.1M NaOH) for 0.3 min, followed by a linear gradient to 4:1 eluent *A*–eluent *B* (0.1M NaOH containing M NaOAc) during 40 min at 4 mL/min and ambient temperature. Fractions were neutralised immediately with M HCl, lyophilised, and desalted on a column (60 × 1 cm) of Bio-Gel P-2 (200–400 mesh, Bio-Rad), followed by a column (10 × 0.5 cm) of Dowex 50W-X8 ($H^+$) resin (100–200 mesh, Bio-Rad) at 4°, and lyophilised.

*Monosaccharide analysis.* — Samples (0.1 mg) were methanolysed (methanolic M HCl, 24 h, 85°) and the resulting methyl glycosides were analysed by g.l.c. of the trimethylsilylated derivatives[14,15] on an SE-30 fused-silica capillary column (25 m × 0.32 mm, Pierce), using a Varian 3700 gas chromatograph connected to a Shimadzu C-R3A recorder/integrator.

*Methylation analysis.* — Samples (0.2 mg) were reduced with $NaBD_4$ (10 mg) in water (2 mL) for 16 h at ambient temperature, the pH was adjusted to 4 by the addition of Dowex 50W-X8 ($H^+$) resin (100–200 mesh) at 4°, and the solution was filtered and lyophilised. Boric acid was removed by evaporation of methanol from the residue under reduced pressure[16]. Methylation analysis of the resulting oligosaccharide-alditols was performed as described[17]. Partially methylated alditol acetates were analysed by g.l.c. on a CPsil 43 WCOT fused-silica capillary column (25 m × 0.32 mm, Chrompack), and by g.l.c.–m.s. on a Carlo–Erba GC/Kratos MS 80/Kratos DS 55 system (electron energy, 70 eV; accelerating voltage, 2.7 kV, ionising current, 100 $\mu$A; CPsil 43 capillary column).

*$^1$H-n.m.r. spectroscopy.* — Samples were repeatedly treated with $D_2O$ (99.9 atom% D, MSD Isotopes), finally using 99.96 atom% D at pD $\geq$7. Resolution-enhanced 500- and 600-MHz $^1$H-n.m.r. spectra were recorded using Bruker AM-500 (Bijvoet Center, Department of NMR Spectroscopy, Utrecht University) and AM-600 (SON-hf-NMR facility, Department of Biophysical Chemistry, Nijmegen University) spectrometers, operating at a probe temperature of 27°. Chemical shifts ($\delta$) are expressed in p.p.m. downfield from the signal for internal sodium 4,4-dimethyl-4-silapentane-1-sulfonate (DSS), but were actually measured by reference to internal acetone ($\delta$ 2.225 in $D_2O$ at 27°)[18] with an accuracy of 0.002 p.p.m.

Homonuclear Hartmann–Hahn (HOHAHA) spin-lock experiments were recorded using the pulse sequence 90°–$t_1$–SL–acq[19–22], wherein SL stands for a multiple of the MLEV-17 sequence. The spin-lock field strength corresponded to a 90° pulse width of 28 $\mu$s and a total spin-lock mixing time of 105 ms. The spectral width was 2994 Hz in each dimension.

Rotating-frame n.O.e. spectroscopy (ROESY) involved the pulse sequence $90_\phi$°–$t_1$–SL–acq[23], where SL stands for a continuous spin-lock pulse of 200 ms at a field strength corresponding to a 90° pulse width between 110–114 $\mu$s. The carrier frequency was placed at the left side of the spectrum at 5.7 p.p.m. in order to minimise HOHAHA-type magnetisation transfer. The HOD signal was suppressed by presaturation during 1.0 s. The spectral width was 3205 Hz in both dimensions.

For both HOHAHA and ROESY spectra, 512 experiments of 4K data points were recorded. The time-proportional phase-increment method (TPPI)[24] was used to create $t_1$ amplitude modulation. The data matrixes were zero-filled to 1K × 8K and multiplied in each time domain with a phase-shifted sine function, shifted $\pi/3$ for the HOHAHA and $\pi/2$ for the ROESY, prior to phase-sensitive F.t.

## RESULTS AND DISCUSSION

*Xylo-oligosaccharides.* — The $^1$H-n.m.r. signals of xylose (**Xyl$_1$**) and xylobiose to xylopentaose (**Xyl$_{2-5}$**), obtained by partial hydrolysis of xylan, were assigned on the basis of 2D HOHAHA and ROESY experiments, except those for H-3,4,5 of the reducing $\alpha$-Xyl*p* residue (Table I). These signals occurred in narrow regions (**Xyl$_1$** $\delta$ 3.58–3.68, **Xyl$_{2-5}$** $\delta$ 3.73–3.82) and there were severe overlap and strong couplings. The signals of the non-reducing end $\beta$-Xyl*p* residue in **Xyl$_{3-5}$** were at higher field than the correspond-

TABLE I

[1]H-N.m.r. data for xylose mono- and oligo-saccharides derived from a (1→4)-β-D-xylan by mild acid hydrolysis

| *Compound*[a] | *Residue*[b] | *Chemical shift*[c] *(coupling constant*[d]*)* | | | | | |
|---|---|---|---|---|---|---|---|
| | | *H-1* | *H-2* | *H-3* | *H-4* | *H-5*eq | *H-5*ax |
| ● | α-Xyl*p* | 5.187 (3.7) | 3.514 (9.4) | 3.58[e] (9.0) | 3.62[e] | 3.68[e] (7.5) | 3.67[e] (7.5) |
| **Xyl$_1$** (Xylose) | β-Xyl*p* | 4.569 (7.9) | 3.218 (9.3) | 3.423 (9.2) | 3.617 | 3.921 (5.5) | 3.314 (10.5, −11.6) |
| ●–● | α-Xyl*p*-**1** | 5.184 (3.6) | 3.545 (9.3) | 3.73–3.82 | | | |
| **Xyl$_2$** (Xylobiose) | β-Xyl*p*-**1** | 4.584 (7.9) | 3.249 (9.4) | 3.547 (9.1) | 3.776 | 4.055 (5.3) | 3.378 (10.5, −11.7) |
| | β-Xyl*p*-**2**$_\alpha$ | 4.453 (7.9) | 3.263 (9.4) | 3.428 (9.1) | 3.628 | 3.972 (5.5) | 3.307 (10.5, −11.7) |
| | β-Xyl*p*-**2**$_\beta$ | 4.457 (7.9) | 3.255 (9.4) | 3.426 (9.1) | 3.625 | | |
| ●–●–● | α-Xyl*p*-**1** | 5.184 (3.6) | 3.545 (9.4) | 3.73–3.82 | | | |
| **Xyl$_3$** (Xylotriose) | β-Xyl*p*-**1** | 4.584 (7.9) | 3.249 (9.4) | 3.548 (9.2) | 3.777 | 4.055 (5.4) | 3.378 (10.4, −11.8) |
| | β-Xyl*p*-**2**$_\alpha$ | 4.476 (7.8) | 3.299 (9.4) | 3.555 (9.2) | 3.785 | 4.107 (5.3) | 3.378 (10.4, −11.8) |
| | β-Xyl*p*-**2**$_\beta$ | 4.479 (7.8) | 3.291 (9.4) | 3.553 (9.2) | 3.787 | | |
| | β-Xyl*p*-**3** | 4.460 (7.8) | 3.256 (9.4) | 3.428 (9.2) | 3.625 | 3.971 (5.4) | 3.307 (10.6, −11.7) |
| ●–●–●–● | α-Xyl*p*-**1** | 5.183 (3.7) | 3.545 (9.4) | 3.73–3.82 | | | |
| **Xyl$_4$** (Xylotetraose) | β-Xyl*p*-**1** | 4.584 (7.9) | 3.249 (9.4) | 3.548 (9.2) | 3.778 | 4.055 (5.4) | 3.378 (10.4, −11.8) |
| | β-Xyl*p*-**2**$_\alpha$ | 4.476 (7.8) | 3.299 (9.4) | | | | |
| | β-Xyl*p*-**2**$_\beta$ | 4.479 (7.8) | 3.291 (9.4) | 3.555 (9.2) | 3.788 | 4.106 (5.3) | 3.378 (10.4, −11.8) |
| | β-Xyl*p*-**3** | 4.482 (7.8) | 3.293 (9.4) | | | | |
| | β-Xyl*p*-**4** | 4.460 (7.9) | 3.256 (9.4) | 3.428 (9.2) | 3.625 | 3.971 (5.4) | 3.307 (10.5, −11.7) |

| | | | | | | | |
|---|---|---|---|---|---|---|---|
| ●–●–●–●–● | α-Xyl*p*-**1** | 5.183 (3.7) | 3.545 (9.4) | 3.73–3.82 | | | |
| **Xyl$_5$** (Xylopentaose) | β-Xyl*p*-**1** | 4.584 (7.9) | 3.249 (9.4) | 3.548 (9.2) | 3.778 | 4.055 (5.4) | 3.378 (10.4, −11.8) |
| | β-Xyl*p*-**2**$_\alpha$ | 4.476 (7.8) | 3.299 (9.4) | | | | |
| | β-Xyl*p*-**2**$_\beta$ | 4.478 (7.8) | | 3.555 (9.2) | 3.788 | 4.106 (5.3) | 3.378 (10.4, −11.8) |
| | β-Xyl*p*-**3** | | 3.292 (9.4) | | | | |
| | | 4.482 (7.8) | | | | | |
| | β-Xyl*p*-**4** | | | | | | |
| | β-Xyl*p*-**5** | 4.459 (7.9) | 3.256 (9.4) | 3.428 (9.2) | 3.625 | 3.971 (5.4) | 3.307 (10.5, −11.7) |

[a] Compounds are represented by short-hand symbolic notation: ●, Xyl*p*; ●–●, β-Xyl*p*-(1→4)-Xyl*p*; *etc.* [b] The Xyl*p* residue in the reducing position is denoted 1, *etc.*; **2**$_\alpha$ and **2**$_\beta$ mean that the reducing Xyl*p*-**1** residue is α or β. [c] In p.p.m. relative to the signal of internal sodium 4,4-dimethyl-4-silapentane-1-sulfonate (using internal acetone at δ 2.225) in $D_2O$ at 27°, acquired at 500 MHz. [d] Observed first-order coupling in Hz. [e] Data taken from ref. 25.

ing signals of the internal β-Xyl*p* residues. Because of the α and β forms of Xyl*p*-**1**, the H-1,2 signals of β-Xyl*p*-**2** (**Xyl$_{2-5}$**) were doubled (*cf.* Table I). For **Xyl$_2$** and **Xyl$_3$**, a doubling was observed for the H-3,4 signals of β-Xyl*p*-**2**. The $^1$H-n.m.r. spectra of oligosaccharides with a d.p. >4 revealed that the signals belonging to the internal residues, except the H-1,2 signals of β-Xyl*p*-**2**, had the same chemical shifts. The first-order coupling constants of the β-Xyl*p* residues indicated the $^4C_1$ chair conformations.

*Arabinoxylan oligosaccharides.* — The mixture of oligosaccharides, obtained by digestion of arabinoxylan with endo-(1→4)-β-D-xylanase, was fractionated on Bio-Gel P-6 (Fig. 1), to give fractions **1–10**. Fraction **1** was shown by h.p.a.e.–p.a.d. to contain Ara and **Xyl$_1$–Xyl$_3$**, and fraction **2** to contain **Xyl$_1$–Xyl$_5$**. In addition, an arabinosylxylotriose was detected in fraction **2** (data not shown). H.p.a.e.–p.a.d. (Fig. 2) of fraction **3** gave two major fractions, **31** (30%) and **33** (41%), and two minor fractions, **32** (13%) and **34** (10%). Data on **31–34** obtained from positive-ion f.a.b.-m.s., monosaccharide analysis, and methylation analysis are presented in Table II. The oligosaccharides in **31** and **32** contained xylotetra- and penta-ose cores, respectively, with an internal Xyl*p* 3-substituted by a single Ara*f* residue. The oligosaccharides in **33** and **34** contained the same cores as in **31** and **32**, respectively, but with an internal Xyl*p* 2,3-substituted by single Ara*f* residues. The primary structures of **31–34** were elucidated further by $^1$H-n.m.r. spectroscopy.

*Fraction* **31**. — The intensities of the signals for anomeric protons in the $^1$H-n.m.r. spectrum of **31** (Fig. 3A) indicated[10] the presence of a single arabinosylxylotetraose, **AX-31** with the Xyl*p* units β ($J_{1,2}$ 7–8 Hz) and the Ara*f* units α ($J_{1,2}$ ~1 Hz). On the various H-1 tracks of the constituent monosaccharides in the 2D HOHAHA spectrum (Fig. 4), the total scalar-coupled networks of each residue were observed, and the data obtained are summarised in Table III. Specific assignment of the α-Ara*f* H-5*proR*,5*proS* signals was based on their relative chemical shifts ($\delta_{5proR} > \delta_{5proS}$) supported by the $J_{4,5}$ values ($J_{4,5proR} < J_{4,5proS}$)[26]. The ROESY spectrum is presented in Fig. 5 and the observed n.O.e.s along the H-1 tracks are compiled in Table IV. The n.O.e.s between H-1 of

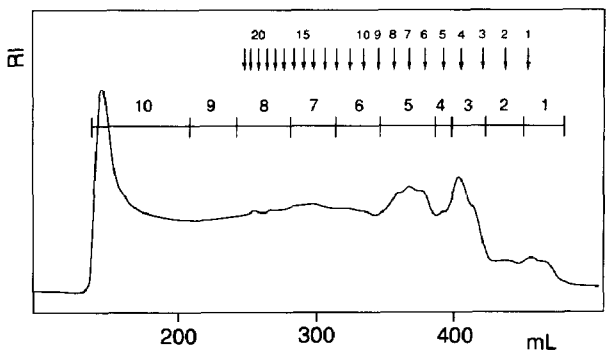


Fig. 1. Bio-Gel P-6 elution profile of oligosaccharides obtained by incubation of arabinoxylan with endo-(1→4)-β-D-xylanase. The arrows at the top indicate the elution position of gluco-oligosaccharides generated by the hydrolysis of dextran, and the associated numbers indicate the d.p.

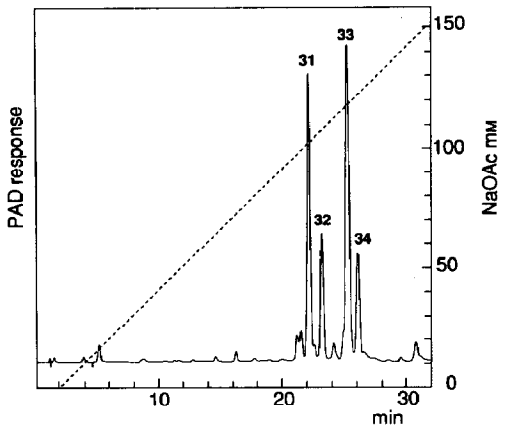


Fig. 2. H.p.a.e.–p.a.d. elution profile of fraction 3 from Fig. 1 on a CarboPac PA-1 column.

TABLE II

Molecular weight and number of pentose residues (in parentheses) as determined by positive-ion f.a.b.-m.s., monosaccharide analysis data, and methylation analysis data for the four h.p.a.e.–p.a.d. fractions derived from fraction 3 in Fig. 1

| | 31 | 32 | 33 | 34 |
|---|---|---|---|---|
| Mol. wt. | 678 (5) | 810 (6) | 810 (6) | 942 (7) |
| *Monosaccharide*[a] | | | | |
| Ara | 1.0 | 1.0 | 2.0 | 2.0 |
| Xyl | 4.0 | 5.1 | 4.1 | 5.2 |
| *Partially methylated alditol acetates*[b] | | | | |
| 2,3,5-$Me_3$-Ara[c] | 0.7 | 0.9 | 2.3 | 2.2 |
| 1,2,3,5-$Me_4$-Xyl[d] | 0.1 | 0.2 | 0.3 | 0.3 |
| 2,3,4-$Me_3$-Xyl | 0.9 | 0.9 | 0.9 | 0.7 |
| 2,3-$Me_2$-Xyl | 0.9 | 1.9 | 1.4 | 2.7 |
| 2-Me-Xyl | 1.0[e] | 1.0[e] | + | 0.2[f] |
| Xyl | – | – | 1.0[e] | 1.0[e] |

[a] Expressed as molar ratios relative to Ara. [b] Molar ratios. [c] 2,3,5-$Me_3$-Ara = 1,4-di-*O*-acetyl-2,3,5-tri-*O*-methyl-arabinitol, *etc.*. [d] Because of the relatively high volatility of this residue, the value is lower than expected. [e] Taken as 1.0. [f] Both 2-Me-Xyl and 3-Me-Xyl were identified in fraction **34**; the presence of 3-Me-Xyl can be explained by undermethylation.

*β*-Xyl*p*-(**n**) and H-4,5*eq* of *β*-Xyl*p*-(**n**−**1**), together with the connectivity between α-Ara*f*-**A**$^{3X3}$ H-1 and *β*-Xyl*p*-**3**$^{II}$ H-3 establish the sequence of **AX-31**.

Comparison of the data for **AX-31** with those of **Xyl**$_4$ (Fig. 3B and Table I) shows nearly identical sets of chemical shifts for *β*-Xyl*p*-**1** and *β*-Xyl*p*-**2**. Owing to the 3-substitution of *β*-Xyl*p*-**3**$^{II}$ by α-Ara*f*-**A**$^{3X3}$, the signals of *β*-Xyl*p*-**3**$^{II}$ are shifted downfield,

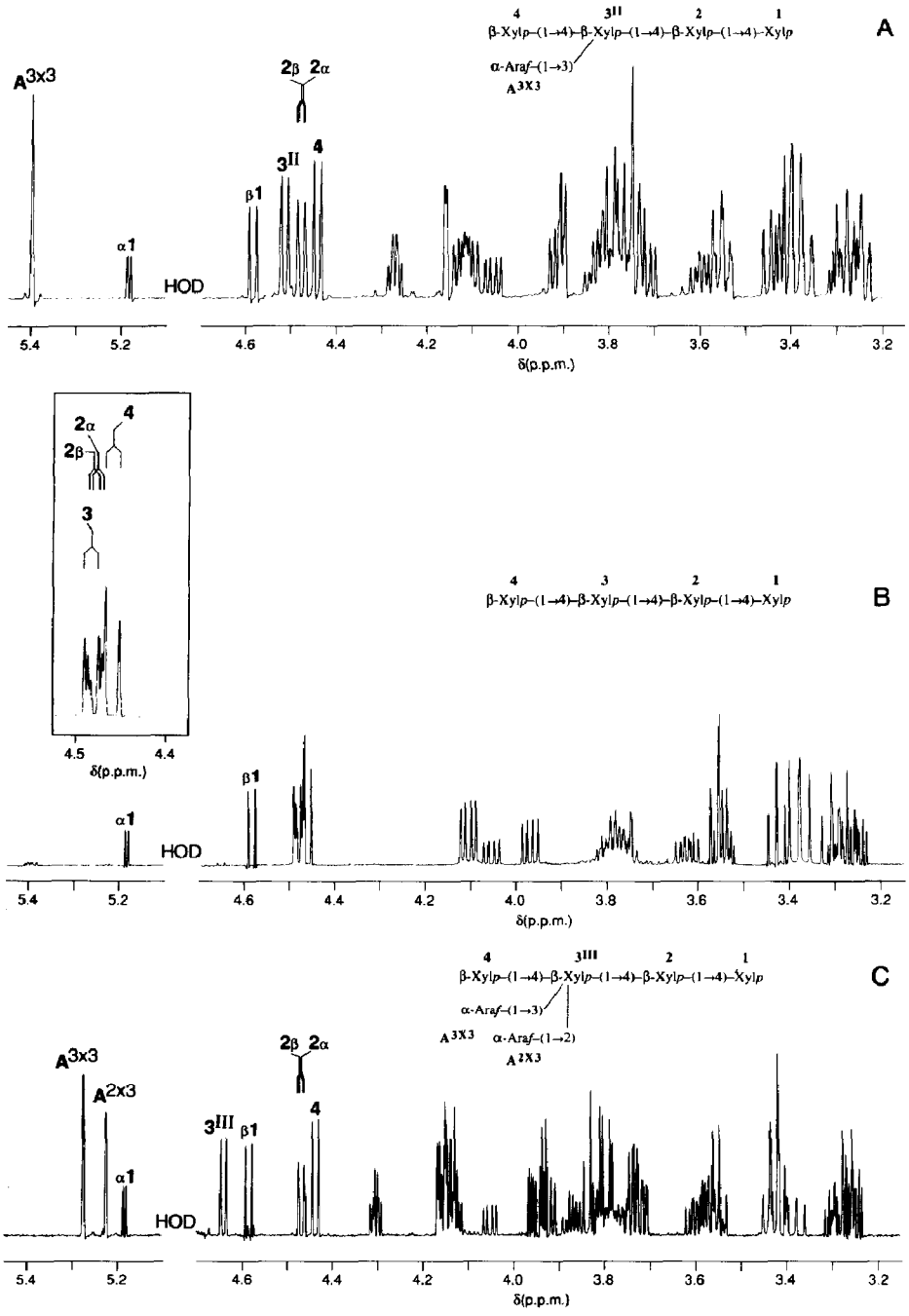


Fig. 3. Resolution-enhanced 500-MHz $^1$H-n.m.r. spectra of fraction **31** (A) and **Xyl$_4$** (B), and the 600-MHz $^1$H-n.m.r. spectrum of fraction **33** (C). In B, the inset shows the expanded region for anomeric protons. The numbers and letters in the spectrum refer to the corresponding residues in the structure.

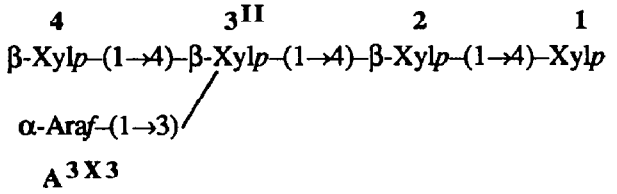


(AX-31)

especially those of H-2 and H-3 ($\Delta\delta$ +0.151 and +0.194, respectively), whereas the signals of $\beta$-Xyl*p*-**4** are shifted slightly upfield.

*Fraction* **33**. — The intensities of the signals for anomeric protons in the $^1$H-n.m.r. spectrum of **33** (Fig. 3C) indicated[10] the presence of a single diarabinosylxylotetraose, **AX-33** with the Xyl*p* units $\beta$ ($J_{1,2}$ 7–8 Hz) and the Ara*f* units $\alpha$ ($J_{1,2}$ ~1 Hz). On the various H-1 tracks of the constituent monosaccharides in the 2D HOHAHA spectrum (Fig. 6), the total scalar-coupled networks of each residue were observed, and the data obtained are summarised in Table III. The ROESY spectrum is presented in Fig. 7 and the observed n.O.e.s along the H-1 tracks are compiled in Table IV. The n.O.e.s between H-1 of $\beta$-Xyl*p*-(**n**) and H-4,5*eq* of $\beta$-Xyl*p*-(**n**−**1**), together with the connectivities

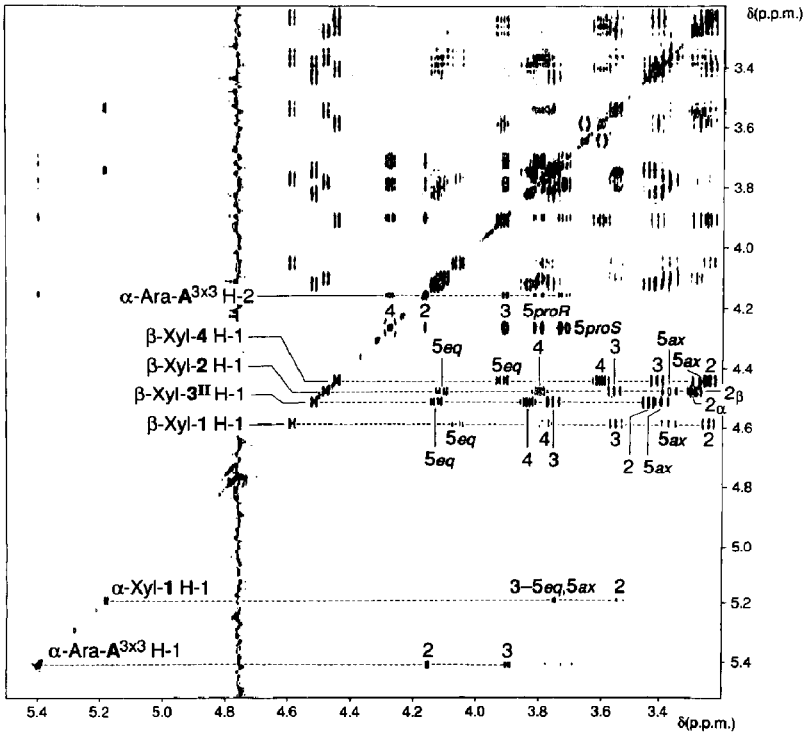


Fig. 4. 600-MHz HOHAHA spectrum of fraction **31**. Diagonal peaks of relevant protons are indicated. The numbers near cross-peaks refer to the protons of the scalar-coupling network belonging to a diagonal peak.

TABLE III

$^{1}$H-N.m.r. data for the arabinoxylan penta- to hepta-saccharides derived from enzymatically degraded wheat arabinoxylan

| *Compound*[a] | *Residue*[b] | *Chemical shift*[c] *(coupling constant*[d]*)* | | | | | |
|---|---|---|---|---|---|---|---|
| | | *H-1* | *H-2* | *H-3* | *H-4* | *H-5*eq/*H-5*proR | *H-5*ax/*H-5*proS |
|  AX-31 | α-Xyl*p*-**1** | 5.184 (3.7) | 3.545 | | | 3.73–3.82 | |
| | β-Xyl*p*-**1** | 4.584 (7.9) | 3.249 (9.4) | 3.548 (9.3) | 3.778 | 4.055 (5.4) | 3.378 (10.4, −11.7) |
| | β-Xyl*p*-**2**$_{\alpha}$ | 4.475 (7.7) | 3.302 (9.4) | 3.554 (9.3) | 3.793 | 4.106 (5.3) | 3.374 (10.4, −11.8) |
| | β-Xyl*p*-**2**$_{\beta}$ | 4.478 (7.7) | 3.291 (9.3) | 3.552 (9.3) | | | |
| | β-Xyl*p*-**3**$^{II}$ | 4.514 (7.8) | 3.444 (9.0) | 3.749 (9.2) | 3.831 | 4.123 (5.2) | 3.402 (10.4, −11.8) |
| | β-Xyl*p*-**4** | 4.442 (7.9) | 3.245 (9.4) | 3.415 (9.3) | 3.596 | 3.913 (5.5) | 3.278 (10.6, −11.6) |
| | α-Ara*f*-**A**$^{3X3}$ | 5.397 (~1.0) | 4.160 (2.4) | 3.907 (5.2) | 4.272 | 3.798 (3.7) | 3.717 (5.8, −12.2) |
|  AX-33 | α-Xyl*p*-**1** | 5.184 (3.7) | 3.546 | | | 3.73–3.82 | |
| | β-Xyl*p*-**1** | 4.585 (7.9) | 3.250 (9.0) | 3.548 (9.2) | 3.774 | 4.053 (5.3) | 3.378 (10.5, −11.7) |
| | β-Xyl*p*-**2**$_{\alpha}$ | 4.466 (7.7) | 3.300 (9.5) | 3.562 (9.3) | 3.793 | 4.146 (5.3) | 3.418 (10.2, −11.8) |
| | β-Xyl*p*-**2**$_{\beta}$ | 4.468 (7.7) | 3.292 (9.5) | | | | |
| | β-Xyl*p*-**3**$^{III}$ | 4.640 (7.1) | 3.572 (8.5) | 3.832 (8.7) | 3.875 | 4.145 (4.5) | 3.434 (8.3, −12.0) |
| | β-Xyl*p*-**4** | 4.436 (7.8) | 3.255 (9.0) | 3.420 (9.3) | 3.602 | 3.924 (5.5) | 3.277 (10.0, −11.5) |
| | α-Ara*f*-**A**$^{2X3}$ | 5.224 (~1.0) | 4.150 (2.7) | 3.959 (6.3) | 4.130 | 3.818 (3.0) | 3.722 (5.4, −12.0) |
| | α-Ara*f*-**A**$^{3X3}$ | 5.274 (~1.0) | 4.167 (2.0) | 3.936 (5.5) | 4.305 | 3.798 (3.0) | 3.724 (5.2, −12.5) |
| 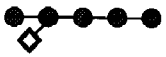 AX-32a | α-Xyl*p*-**1** | 5.184 | 3.544 | | | 3.73–3.82 | |
| | β-Xyl*p*-**1** | 4.584 | 3.248 | 3.547 | 3.779 | 4.055 | 3.378 |
| | β-Xyl*p*-**2** | 4.478 | 3.290 | 3.553 | 3.790 | 4.105 | 3.375 |
| | β-Xyl*p*-**3** | 4.482 | | | | | |
| | β-Xyl*p*-**4**$^{II}$ | 4.514 | 3.441 | 3.748 | 3.831 | 4.122 | 3.400 |
| | β-Xyl*p*-**5** | 4.442 | 3.245 | 3.415 | 3.595 | 3.911 | 3.279 |
| | α-Ara*f*-**A**$^{3X4}$ | 5.396 | 4.158 | 3.904 | 4.273 | 3.799 | 3.716 |

| | | | | | | | |
|---|---|---|---|---|---|---|---|
| 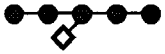 | α-Xyl*p*-1 | 5.184 | 3.544 | | | 3.73–3.82 | |
| | β-Xyl*p*-1 | 4.584 | 3.248 | 3.547 | 3.779 | 4.055 | 3.378 |
| | β-Xyl*p*-2 | 4.478 | 3.290 | 3.553 | 3.790 | 4.105 | 3.375 |
| **AX-32b** | β-Xyl*p*-3$^{II}$ | 4.514 | 3.441 | 3.744 | 3.829 | 4.122 | 3.400 |
| | β-Xyl*p*-4 | 4.461 | 3.277 | 3.538 | 3.752 | 4.049 | 3.343 |
| | β-Xyl*p*-5 | 4.448 | 3.248 | 3.428 | 3.620 | 3.965 | 3.297 |
| | α-Ara*f*-A$^{3X3}$ | 5.391 | 4.160 | 3.912 | 4.273 | 3.799 | 3.720 |
| 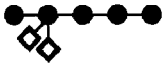 | α-Xyl*p*-1 | 5.183 | 3.544 | | | 3.73–3.82 | |
| | β-Xyl*p*-1 | 4.584 | 3.247 | 3.546 | 3.770 | 4.053 | 3.378 |
| | β-Xyl*p*-2 | 4.478 | 3.289 | 3.552 | 3.783 | 4.102 | 3.378 |
| **AX-34a** | β-Xyl*p*-3 | 4.472 | 3.290 | 3.562 | 3.791 | 4.144 | 3.420 |
| | β-Xyl*p*-4$^{III}$ | 4.639 | 3.571 | 3.829 | 3.874 | 4.144 | 3.432 |
| | β-Xyl*p*-5 | 4.437 | 3.254 | 3.418 | 3.599 | 3.922 | 3.278 |
| | α-Ara*f*-A$^{2X4}$ | 5.225 | 4.149 | 3.959 | 4.126 | 3.817 | 3.721 |
| | α-Ara*f*-A$^{3X4}$ | 5.273 | 4.166 | 3.934 | 4.306 | 3.797 | 3.725 |
|  | α-Xyl*p*-1 | 5.183 | 3.544 | | | 3.73–3.82 | |
| | β-Xyl*p*-1 | 4.584 | 3.247 | 3.546 | 3.770 | 4.053 | 3.378 |
| **AX-34b** | β-Xyl*p*-2 | 4.468 | 3.290 | 3.562 | 3.791 | 4.144 | 3.420 |
| | β-Xyl*p*-3$^{III}$ | 4.639 | 3.571 | 3.829 | 3.874 | 4.144 | 3.432 |
| | β-Xyl*p*-4 | 4.455 | 3.253 | 3.542 | 3.753 | 4.062 | 3.340 |
| | β-Xyl*p*-5 | 4.451 | 3.249 | 3.420 | 3.622 | 3.968 | 3.289 |
| | α-Ara*f*-A$^{2X3}$ | 5.225 | 4.149 | 3.959 | 4.126 | 3.817 | 3.721 |
| | α-Ara*f*-A$^{3X3}$ | 5.273 | 4.166 | 3.943 | 4.306 | 3.797 | 3.725 |

[a] Compounds are represented by short-hand symbolic notation: ●, Xyl*p*: ◇, α-Ara*f*; ◇●, α-Ara*f*-(1→2)-β-Xyl*p*; ◇●, α-Ara*f*-(1→3)-β-Xyl*p*. [b] The Xyl*p* residue in the reducing position is denoted 1, *etc.*; $2_\alpha$ and $2_\beta$ mean that the reducing Xyl*p*-1 residue is α or β. Ara*f*-A$^{2X3}$ means arabinofuranose linked to O-2 of Xyl*p*-3, *etc.*, Xyl*p*-3$^{I}$ means Xyl*p*-3 branched at O-2, Xyl*p*-3$^{II}$ means Xyl*p*-3 branched at O-3, Xyl*p*-3$^{III}$ means Xyl*p*-3 branched at O-2,3. [c] In p.p.m. relative to the signal of internal sodium 4,4-dimethyl-4-silapentane-1-sulfonate (using internal acetone at δ 2.225) in $D_2O$ at 27°, acquired at 600 MHz (**AX-31** at 500 MHz). [d] Observed first-order couplings in Hz.

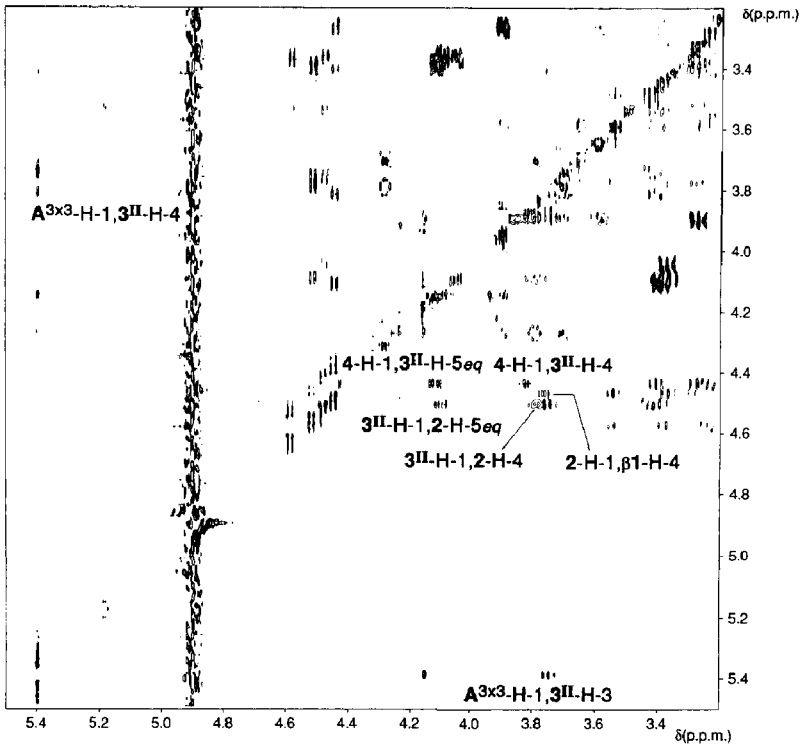


Fig. 5. 600-MHz ROESY spectrum of fraction **31**. Only the inter-residue n.O.e. connectivities along the H-1 tracks are denoted and only the negative levels are given. $A^{3X3}$ means α-Ara*f* 3-linked to β-Xyl*p*-**3**; $A^{3X3}$-H-1,$3^{II}$-H-3 means the cross-peak between H-1 of α-Ara*f*-$A^{3X3}$ and H-3 of β-Xyl*p*-$3^{II}$, *etc.*.

α-Ara*f*-$A^{2X3}$ H-1,β-Xyl*p*-$3^{III}$ H-2 and α-Ara*f*-$A^{3X3}$ H-1,β-Xyl*p*-$3^{III}$ H-3 established the sequence of **AX-33**.

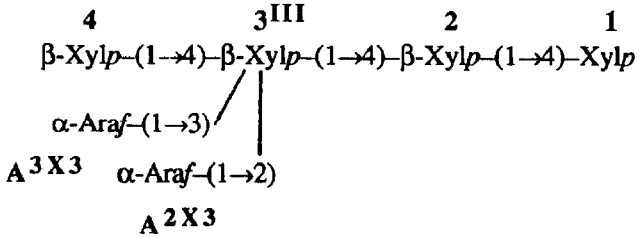


**(AX-33)**

Comparison of the $^1$H-n.m.r. data of **AX-33** with those of **AX-31** (Table III) shows significant downfield shifts of the β-Xyl*p*-$3^{III}$ H-1,2,3 signals compared to those of β-Xyl*p*-$3^{II}$ H-1,2,3, in accordance with the 2,3-glycosylation of β-Xyl*p*-$3^{III}$. The inter-residue connectivities $A^{2X3}$-H-1,$A^{3X3}$-H-2 and $A^{3X3}$-H-1,$A^{2X3}$-H-2 can be explained on basis of the 3D structure. The 2,3-glycosylation of β-Xyl*p*-$3^{III}$ by α-Ara*f* residues affected

TABLE IV

Cross-peaks observed at the H-1 tracks in the ROESY spectra of arabinoxylan penta-to hepta-saccharides, measured with a mixing time of 200 ms

| *Compound* | *Residue* | *N.O.e. effect* |
|---|---|---|
| **AX-31** | Xyl-**2** H-1 | Xyl-**2** H-3,5*ax*; Xyl-**1**β H-4,5*eq* |
| | Xyl-**3**$^{II}$ H-1 | Xyl-**3**$^{II}$ H-3,5*ax*; Xyl-**2** H-4,5*eq* |
| | Xyl-**4** H-1 | Xyl-**4** H-3,5*ax*; Xyl-**3**$^{II}$ H-4,5*eq* |
| | Ara-A$^{3X3}$ H-1 | Ara-A$^{3X3}$ H-2; Xyl-**3**$^{II}$ H-3,4(very weak) |
| **AX-33** | Xyl-**2** H-1 | Xyl-**2** H-3,5*ax*; Xyl-**1**β H-4,5*eq*(very weak); Xyl-**1**α H-4 |
| | Xyl-**3**$^{III}$ H-1 | Xyl-**3**$^{III}$ H-3,5*ax*; Xyl-**2** H-4,5*eq* |
| | Xyl-**4** H-1 | Xyl-**4** H-3,5*ax*; Xyl-**3**$^{III}$ H-3$^a$,4,5*eq* |
| | Ara-A$^{2X3}$ H-1 | Ara-A$^{2X3}$ H-2; Ara-A$^{3X3}$ H-2; Xyl-**3**$^{III}$ H-2 |
| | Ara-A$^{3X3}$ H-1 | Ara-A$^{3X3}$ H-2; Ara-A$^{2X3}$ H-2; Xyl-**3**$^{III}$ H-3,4(weak)$^a$ |
| **AX-32a** | Xyl-**2** H-1 | Xyl-**2** H-3,5*ax*; Xyl-**1**β H-4,5*eq*; Xyl-**1**α H-4,5 |
| | Xyl-**3** H-1 | Xyl-**3** H-3,5*ax*; Xyl-**2** H-4,5*eq* |
| | Xyl-**4**$^{II}$ H-1 | Xyl-**4**$^{II}$ H-3,5*ax*; Xyl-**3** H-4,5*eq* |
| | Xyl-**5** H-1 | Xyl-**5** H-5*ax*; Xyl-**4**$^{II}$ H-4,5*eq* |
| | Ara-A$^{3X4}$ H-1 | Ara-A$^{3X4}$ H-2; Xyl-**4**$^{II}$ H-3 |
| **AX-32b** | Xyl-**2** H-1 | Xyl-**2** H-3,5*ax*; Xyl-**1**β H-4,5*eq*; Xyl-**1**α H-4,5 |
| | Xyl-**3**$^{II}$ H-1 | Xyl-**3**$^{II}$ H-3,5*ax*; Xyl-**2** H-4,5*eq* |
| | Xyl-**4** H-1 | Xyl-**4** H-3(weak), 5*ax*; Xyl-**3**$^{II}$ H-4,5*eq* |
| | Xyl-**5** H-1 | Xyl-**5** H-5*ax*; Xyl-**4** H-4,5*eq* |
| | Ara-A$^{3X3}$ H-1 | Ara-A$^{3X3}$ H-2; Xyl-**3**$^{II}$ H-3 |
| **AX-34a** | Xyl-**2** H-1 | Xyl-**2** H-3,5*ax*; Xyl-**1**β H-4,5*eq*(very weak); Xyl-**1**α H-4,5 |
| | Xyl-**3** H-1 | Xyl-**3** H-3,5*ax*; Xyl-**2** H-4,5*eq* |
| | Xyl-**4**$^{III}$ H-1 | Xyl-**4**$^{III}$ H-3,5*ax*; Xyl-**3** H-4,5*eq* |
| | Xyl-**5** H-1 | Xyl-**5** H-3,5*ax*; Xyl-**4**$^{III}$ H-4,5*eq* |
| | Ara-A$^{2X4}$ H-1 | Ara-A$^{2X4}$ H-2; Ara-A$^{3X4}$ H-2; Xyl-**4**$^{III}$ H-2 |
| | Ara-A$^{3X4}$ H-1 | Ara-A$^{3X4}$ H-2; Ara-A$^{2X4}$ H-2; Xyl-**4**$^{III}$ H-3,4(weak)$^a$ |
| **AX-34b** | Xyl-**2** H-1 | Xyl-**2** H-3,5*ax*; Xyl-**1**β H-4,5*eq*; Xyl-**1**α H-4,5 |
| | Xyl-**3**$^{III}$ H-1 | Xyl-**3**$^{III}$ H-3,5*ax*; Xyl-**2** H-4,5*eq* |
| | Xyl-**4** H-1 | Xyl-**4** H-5*ax*; Xyl-**3**$^{III}$ H-4,5*eq* |
| | Xyl-**5** H-1 | Xyl-**5** H-5*ax*; Xyl-**4** H-4,5*eq* |
| | Ara-A$^{2X3}$ H-1 | Ara-A$^{2X3}$ H-2; Ara-A$^{3X3}$ H-2; Xyl-**3**$^{III}$ H-2 |
| | Ara-A$^{3X3}$ H-1 | Ara-A$^{3X3}$ H-2; Ara-A$^{2X3}$ H-2; Xyl-**3**$^{III}$ H-3,4(weak)$^a$ |

$^a$ Cross-peak is a relayed ROESY contact, caused by spin diffusion due to the small chemical shift difference between H-3 and H-4 of the double-branched β-Xyl*p*.

the $^4C_1$ chair conformation, which was reflected by the change in the $^3J$ values of β-Xyl*p*-**3**$^{III}$ relative to those of un- or mono-substituted β-Xyl*p* residues (*cf.* Table III). The small differences in chemical shifts between the signals of β-Xyl*p*-**2** in **AX-33** and **AX-31** may have been due to backfolding of the 2-linked α-Ara*f*-A$^{2X3}$ residue along the xylan-backbone.

The Xyl*p*-(**n**) H-1,Xyl*p*-(**n**−**1**) H-4 and Xyl*p*-(**n**) H-1,Xyl*p*-(**n**−**1**) H-5*eq* n.O.e.s in the ROESY spectrum of **AX-33** (and also in that of **AX-31**) had comparable signal

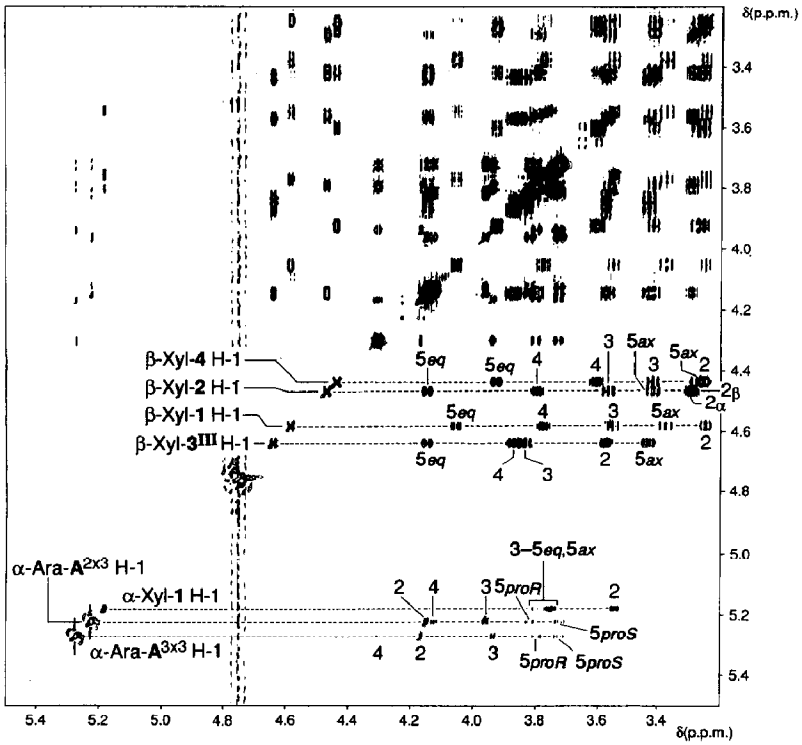


Fig. 6. 600-MHz HOHAHA spectrum of fraction **33**. Diagonal peaks of the anomeric protons are indicated. The numbers near cross-peaks refer to the protons of the scalar-coupling network belonging to a diagonal peak.

intensities, which suggested that *β*-Xyl*p*-(**n**) H-1 was positioned at similar distances from *β*-Xyl*p*-(**n**−1) H-4,5*eq*, so that, in solution at 27°, the xylo-oligosaccharides adopted a left-handed three-fold helix conformation in line with that proposed for xylan-hydrate on the basis of X-ray fibre diffraction data[27].

*Fraction* **32**. — The data in Table II indicate that **32** contained hexasaccharide(s) built up from a xylopentaose core with an internal *β*-Xyl*p* residue 3-substituted by one *α*-Ara*f*. The $^1$H-n.m.r. spectrum of **32** (Fig. 8) contains signals with different intensities which indicate that two hexasaccharides were present. Two *α*-Ara*f* H-1 signals are present at *δ* 5.396 and 5.391, with relative intensities of 2:3. In the region for anomeric protons, the *β*-Xyl*p* H-1 signals of **AX-31** are observed but they have different intensities with that at *δ* 4.442 being lower. Additional signals are present at *δ* 4.448, 4.461, and 4.482. The H-1 signals at *δ* 4.442 and 4.482 have the same intensities as the *α*-Ara*f*-**A**$^{3X4}$ H-1 signal at *δ* 5.396. The combined HOHAHA and ROESY data (Tables III and IV, respectively) show that the signals at *δ* 4.442 and 5.396 stemmed from the same terminal sequence as in **AX-31**, *i.e.* *β*-Xyl*p*-**4**(*α*-Ara*f*-**A**$^{3X3}$)*β*-Xyl*p*-**3**$^{II}$, denoted *β*-Xyl*p*-**5**(*α*-Ara*f*-**A**$^{3X4}$)*β*-Xyl*p*-**4**$^{II}$ in structure **AX-32a** (see below). The ROESY data showed that this terminal sequence was not linked to a reducing xylobiose unit, as in **AX-31**, but to a

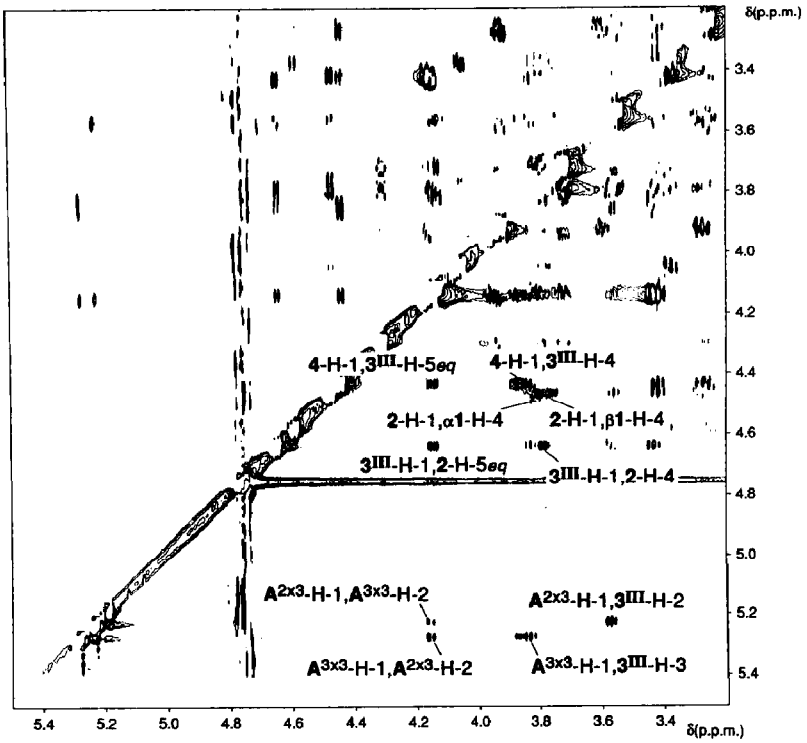


Fig. 7. 600-MHz ROESY spectrum of fraction **33**. Only the inter-residue n.O.e. connectivities along the H-1 tracks are denoted and only the negative levels are given. $A^{3x3}$-H-1,$3^{III}$-H-3 means the cross-peak between H-1 of α-Ara*f*-$A^{3x3}$ and H-3 of β-Xyl*p*-$3^{III}$, *etc.*

reducing xylotriose unit, as is evident from the additional H-1 signal at δ 4.482 which stemmed from β-Xyl*p*-**3** (*cf.* **Xyl$_4$** and **Xyl$_5$**; Table I). The signals of β-Xyl*p*-**1,2** have the same chemical shifts as those of the corresponding residues in **AX-31** and **Xyl$_4$**. Based on the $^1$H-n.m.r. data, the structure of the minor component (**AX-32a**) of fraction **32** is

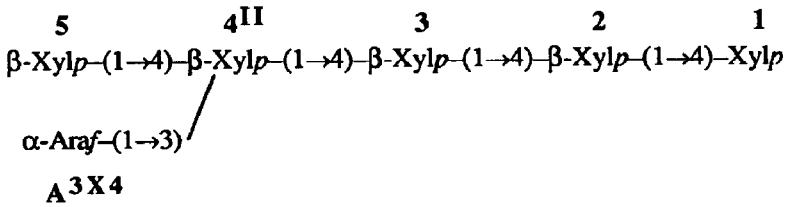


**(AX-32a)**

The major arabinosylxylopentaose contained a terminal unbranched xylobiosyl group at the non-reducing end, characterised by the H-1 signals at δ 4.448 and 4.461 for the terminal and penultimate β-Xyl*p* residues, respectively (Table III). The ROESY data (Table IV) show that the H-1 signal at δ 4.461 has a cross-peak with H-4,5*eq* of the

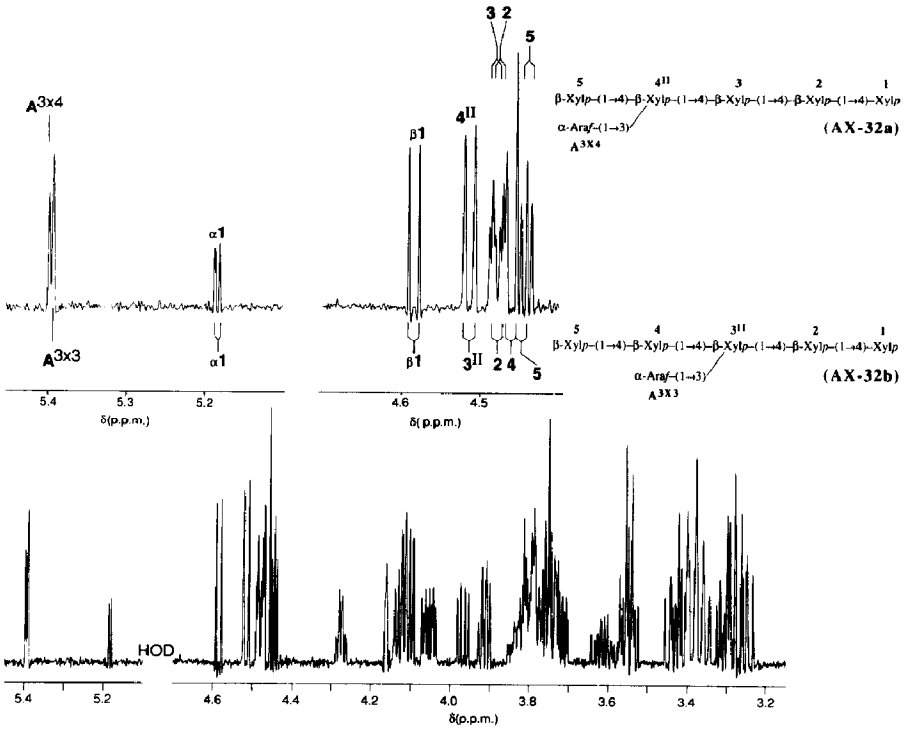


Fig. 8. Resolution-enhanced 600-MHz $^1$H-n.m.r. spectrum of fraction **32**. The inset shows the expanded region for anomeric protons. The numbers and letters in the spectrum refer to the corresponding residues in the structures.

3-branched *β*-Xyl*p* residue. Thus, this non-reducing xylobiosyl group was 4-linked to the branched residue. The intensities of the H-1 signals at $\delta$ 4.448 and 4.461 are identical to that of the α-Ara*f* H-1 signal at $\delta$ 5.391, showing that they are associated with the same oligosaccharide **AX-32b**. The signals of *β*-Xyl*p*-**1,2** have the same chemical shifts as those of the corresponding residues in **AX-31**. Based on the $^1$H-n.m.r. data, the structure of **AX-32b** is

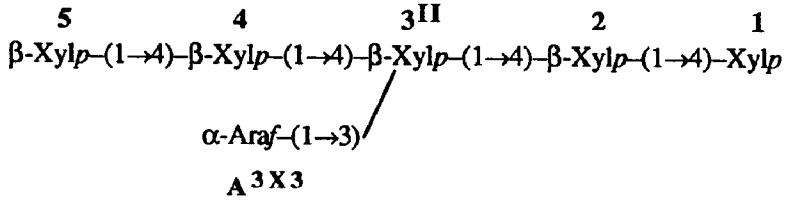


**(AX-32b)**

Exhaustive digestion of fraction **32** with endo-(1→4)-*β*-D-xylanase yielded only one hexasaccharide, the $^1$H-n.m.r. data of which matched completely those of **AX-32b** (Table III).

*Fraction* **34**. — The data in Table II indicate that **34** contained heptasaccharide(s)

built up from a xylopentaose core with an internal β-Xyl*p* residue 2,3-substituted by single α-Ara*f* residues. The $^1$H-n.m.r. spectrum of **34** is presented in Fig. 9. In the region for anomeric protons, all β-Xyl*p* H-1 signals of **AX-33** are observed, but they have different intensities. As deduced from the relative intensities of the β-Xyl*p* H-1 signals at δ 4.437 and 4.451, identified as belonging to two terminal β-Xyl*p* residues, two heptasaccharides were present in about equal amounts. Exhaustive digestion of **34** with endo-(1→4)-β-D-xylanase yielded only one heptasaccharide. This diarabinosylxylopentaose (**AX-34b**) contained a terminal unbranched xylobiosyl group at the non-reducing end, characterised by the H-1 signals at δ 4.451 and 4.455 for the terminal and penultimate β-Xyl*p* residues, respectively, as deduced from the combined HOHAHA and ROESY data of **34** (Tables III and IV, respectively). Furthermore, these data show that the H-1 signal at δ 4.455 has a cross-peak with H-4,5*eq* of a 2,3-branched β-Xyl*p* residue. Thus, this non-reducing xylobiosyl group was 4-linked to the branched residue, denoted β-Xyl*p*-**3**$^{III}$. The signals of β-Xyl*p*-**1,2** have the same chemical shifts as those of the corresponding residues in **AX-33**. Based on the $^1$H-n.m.r. data, the structure of **AX-34b** is

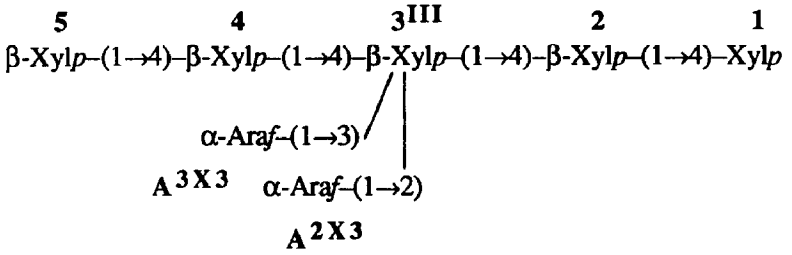


**(AX-34b)**

The second diarabinosylxylopentaose (**AX-34a**) is reflected by H-1 signals at δ 4.472 and 4.478 with intensities similar to that of the terminal β-Xyl*p* H-1 signal at δ 4.437. The HOHAHA and ROESY data of **34** (Tables III and IV, respectively) indicate that the non-reducing terminal tetrasaccharide in **AX-33**, *i.e.* β-Xyl*p*-**4**(α-Ara*f*-**A**$^{2X3}$)(α-Ara*f*-**A**$^{3X3}$)β-Xyl*p*-**3**$^{III}$, was also present in fraction **34**, corresponding to β-Xyl*p*-**5**(α-Ara*f*-**A**$^{2X4}$)(α-Ara*f*-**A**$^{3X4}$)β-Xyl*p*-**4**$^{III}$ of **AX-34a** (see below). These data show also that this non-reducing terminal unit was linked to a xylotriose unit. In particular, the n.O.e. contacts β-Xyl*p*-**4**$^{III}$ H-1,β-Xyl*p*-**3** H-4,5*eq* corroborate this conclusion. The H-1 signals at δ 4.472 and 4.478 are attributed to β-Xyl*p*-**3** and β-Xyl*p*-**2** H-1, respectively. Based on the $^1$H-n.m.r. data, the structure of **AX-34a** is

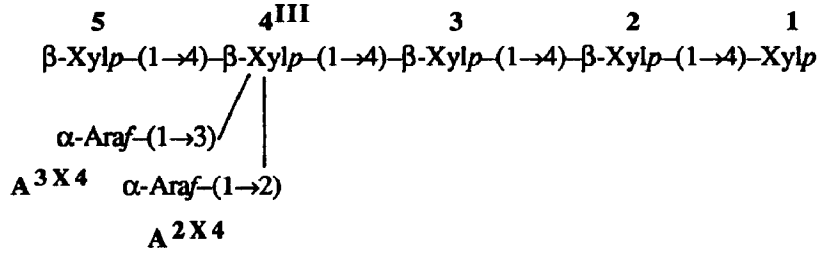


(AX-34a)

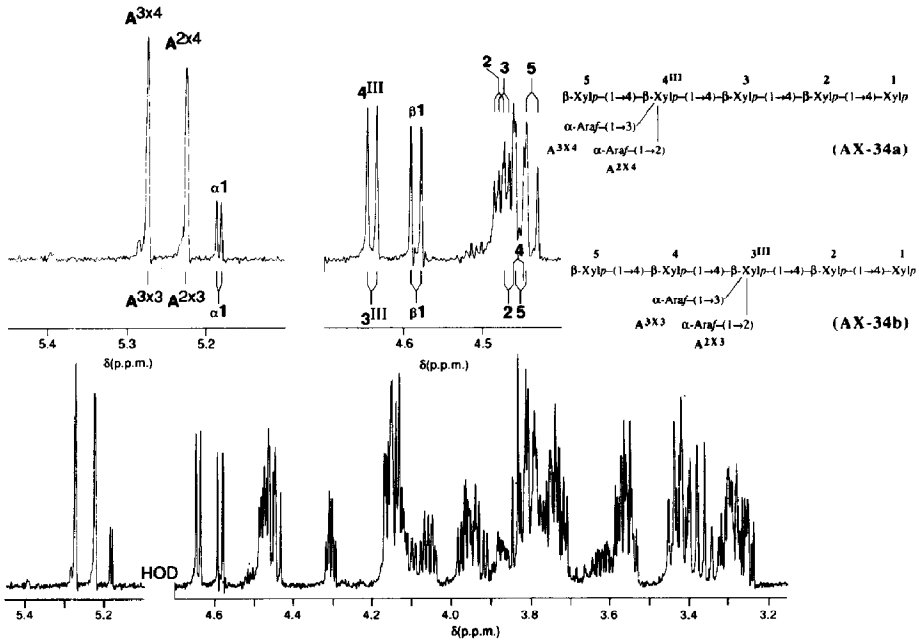


Fig. 9. Resolution-enhanced 600-MHz $^1$H-n.m.r. spectrum of fraction **34**. The inset shows the expanded region for anomeric protons. The numbers and letters in the spectrum refer to the corresponding residues in the structures.

ACKNOWLEDGMENTS

We thank M. Roza and Professor Dr. J. Maat (Unilever Research Laboratory, Vlaardingen) for the kind gift of purified endo-(1→4)-β-D-xylanase and valuable discussion, Professor Dr. B. Fournet (Laboratoire de Spectrométrie de Masse de l'Université des Sciences et Techniques de Lille Flandres-Artois, Villeneuve d'Ascq) for recording the f.a.b.-mass spectra, and A. C. van der Kerk-van Hoof (Laboratory of Analytical Chemistry, Utrecht University) for recording the g.l.c.–m.s. data. This

investigation was carried out with financial aid from Unilever Research Vlaardingen, the Dutch Ministry of Economic Affairs (ITP-program), and the Netherlands Foundation for Chemical Research (NWO/SON).

## REFERENCES

1 J.-M. Brillouet, J.-P. Joseleau, J. P. Uttille, and D. Le-Lievre, *J. Agric. Food Chem.*, 30 (1982) 488–495.
2 R. Amadò and H. Neukom, in R. D. Hill and L. Munch (Eds.), *New Approaches to Research on Cereal Carbohydrates*, Elsevier, Amsterdam, 1985, pp. 241–251.
3 H. Gruppen, J. P. Marseille, A. G. J. Voragen, R. J. Hamer, and W. J. Pilnik, *Cereal Sci.*, 9 (1989) 247–260.
4 G. O. Aspinall and R. C. Carpenter, *Carbohydr. Polym.*, 4 (1984) 271–282.
5 G. M. Ballance, R. S. Hall, and D. J. Manners, *Carbohydr. Res.*, 150 (1986) 290–294.
6 S. Bengtsson and P. Åman, *Carbohydr. Polym.*, 12 (1990) 267–277.
7 N. Shibuya and T. Iwasaki, *Phytochemistry*, 24 (1985) 285–289.
8 D. G. Medcalf and K. A. Gilles, *Cereal Chem.*, 45 (1968) 550–556.
9 R. A. Hoffmann, M. Roza, J. Maat, J. P. Kamerling, and J. F. G. Vliegenthart, *Carbohydr. Polym.*, 16 (1991) 275–289.
10 M. M. Smith and R. D. Hartley, *Carbohydr. Res.*, 118 (1983) 65–80.
11 I. Mueller-Harvey, R. D. Hartley, P. J. Harris, and E. H. Curzon, *Carbohydr. Res.*, 148 (1986) 71–85.
12 A. Kato, J.-I. Azuma, and T. Koshijima, *Agric. Biol. Chem.*, 51 (1987) 1691–1693.
13 S. Huges and D. C. Johnson, *Anal. Chim. Acta*, 132 (1981) 11–22.
14 J. P. Kamerling and J. F. G. Vliegenthart, *Cell Biol. Monogr.*, 10 (1982) 95–125.
15 J. P. Kamerling, G. J. Gerwig, J. F. G. Vliegenthart, and J. R. Clamp, *Biochem. J.*, 151 (1975) 491–495.
16 S. A. M. Korrel, K. J. Clemetson, H. van Halbeek, J. P. Kamerling, J. J. Sixma, and J. F. G. Vliegenthart, *Eur. J. Biochem.*, 140 (1984) 571–576.
17 A. L. Kvernheim, *Acta Chem. Scand., Ser. B*, 41 (1987) 150–152.
18 J. F. G. Vliegenthart, L. Dorland, and H. van Halbeek, *Adv. Carbohydr. Chem. Biochem.*, 41 (1983) 209–374.
19 A. Bax and D. G. Davis, *J. Magn. Reson.*, 65 (1985) 355–360.
20 L. Braunsweiler and R. R. Ernst, *J. Magn. Reson.*, 53 (1983) 521–526.
21 D. G. Davis and A. Bax, *J. Am. Chem. Soc.*, 107 (1985) 2820–2821.
22 M. W. Edwards and A. Bax, *J. Am. Chem. Soc.*, 108 (1986) 918–923.
23 A. Bax and D. G. Davis, *J. Magn. Reson.*, 63 (1985) 207–213.
24 D. Marion and K. Wüthrich, *Biochem. Biophys. Res. Commun.*, 113 (1983) 967–974.
25 K. Bock and H. Thøgersen, *Annu. Rep. NMR Spectrosc.*, 13 (1982) 1–57.
26 G. D. Wu, A. S. Serianni, and R. Baker, *J. Org. Chem.*, 48 (1983) 1750–1757.
27 I. A. Nieduszynski and R. H. Marchessault, *Biopolymers*, 11 (1972) 1335–1344.